Mutation of Arginine 264 on ERα (Estrogen Receptor Alpha) Selectively Abrogates the Rapid Signaling of Estradiol in the Endothelium Without Altering Fertility

Marine Adlanmerini, Chanaëlle Febrissy, Rana Zahreddine, Emilie Vessières, Melissa Buscato, Romain Solinhac, Julie Favre, Typhaine Anquetil, Anne-Laure Guihot, Frederic Boudou, et al.

Mutation of Arginine 264 on Estrogen Receptor α selectively abrogates the rapid signaling of estradiol in the endothelium without altering fertility

M. Adlanmerini[1], C. Febrissy [1], R. Zahreddine[1], E. Vessières[2]; M. Buscato[1], R. Solinhac[1], J. Favre[2]. T. Anquetil[1], A.L. Guihot[2], F. Boudou[1], I. Raymond-Letron[3], P. Chambon[5], P. Gourdy[1], C. Ohlsson[6], H. Laurell[1], C. Fontaine[1], R. Metivier[7], M. Le Romancer[4], D. Henrion[2], J.F. Arnal[1], F. Lenfant[1]

[1]INSERM-UPS UMR U1048, Institut des Maladies Métaboliques et Cardiovasculaires, Université de Toulouse, BP 84225, 31 432 Toulouse cedex 04, France
[2] Institut National de la Santé et de la Recherche Médicale U1083, Centre National de la Recherche Scientifique, Unité Mixte de Recherche 46 015, Université d'Angers, 49000 Angers, France;
[3] Institut National Polytechnique, École Nationale Vétérinaire de Toulouse, Institut National de la Santé et de la Recherche Médicale, Unité Mixte de Service 006, Université de Toulouse, F-31076 Toulouse, France
[4] Inserm U1052, CNRS UMR5286, Centre de Recherche en Cancérologie de Lyon, F-69000 Lyon, France
[5] Institut de Génétique et de Biologie Moléculaire et Cellulaire, Collège de France, Université de Strasbourg, FR-67404 Illkirch, France
[6] Centre for Bone and Arthritis Research Institute of Medicine, The Sahlgrenska Academy, University of Gothenburg, S-41345 Gothenburg, Sweden.
[7] CNRS, Univ Rennes, IGDR (Institut de Génétique De Rennes) – UMR 6290, F-35000 Rennes, France

Corresponding author: francoise.lenfant@inserm.fr
INSERM-UPS UMR U1048, Institut des Maladies Métaboliques et Cardiovasculaires, Université de Toulouse, BP 84225, 31 432 Toulouse cedex 04, France- Tél : (33)-+5-31-22-40-93

Running title : R264-ERα is required for rapid signaling

Word count : 9070 with references

Total number of Figures and Tables: 6 Figures and 2 Tables

Abbreviations: ERα: Estrogen Receptor ERα, E2 (17β-estradiol); NO: Nitric oxide

TOC category: basic studies

TOC subcategory: Vascular Biology

Abstract

Objective:
Estrogen Receptor alpha (ERα) exerts nuclear genomic actions and also rapid membrane-initiated steroid signaling (MISS). The mutation of the cysteine 451 into alanine *in vivo* has recently revealed the key role of this ERα palmitoylation site on some vasculoprotective actions of estradiol and fertility. Here, we studied the *in vivo* role of the arginine 260 of ERα which has also been described to be involved in its E2-induced rapid signaling with PI3-Kinase as well as G protein in cultured cell lines.
Approach and results:
We generated a mouse model harboring a point mutation of the murine counterpart of this arginine into alanine (R264A-ERα). In contrast to the C451A-ERα, the *R264A-ERα* females are fertile with standard hormonal serum levels and normal control of hypothalamus-pituitary ovarian axis. Although R264A-ERα protein abundance was normal, the well-described membrane ERα–dependent actions of estradiol, such as the rapid dilation of mesenteric arteries and the acceleration of endothelial repair of carotid were abrogated in *R264A-ERα* mice. In striking contrast, E2-regulated gene expression was highly preserved in the uterus and in the aorta, revealing intact nuclear/genomic actions in response to E2. Consistently, two recognized nuclear ERα-dependent actions of E2, namely atheroma prevention and flow-mediated arterial remodeling were totally preserved.

Conclusions:
These data underline the exquisite role of Arginine 264 of ERα for endothelial MISS effects of E2, but not for nuclear/genomic actions. This provides the first model of fertile mouse with no overt endocrine abnormalities with specific loss-of-function of rapid ERα signaling in vascular functions.

Introduction

ERα, a member of the nuclear receptor family, is implicated in many physiological processes including reproduction, metabolism or cardio-vascular protection. ERα classically mediates its biological functions through regulation of gene expression via recruitment of cofactors to the AF1 and AF2 transactivation functions. These ERα-induced transcriptional changes occur in a cell- and tissue-specific manner, through either direct DNA interactions with Estrogen-responsive Elements (EREs), or indirectly, through protein-protein tethering with transcription factors such as c-Fos/c-Jun (AP-1) and SP1 [1]. However, besides this traditionally activity acting as a nuclear transcription factor, ERα can also mediate Membrane Initiated Steroid Signaling (MISS), usually termed "nongenomic" or "extranuclear" effects. These rapid effects of estrogen, such as the mobilization of intracellular calcium and generation of cAMP, were first described several decades ago [2, 3]. *In vitro* studies allowed defining more precisely this extranuclear signaling of ERα. In particular, palmitoylation of human Cys447 was found to promote interaction with caveolin-1 and plasma membrane localization [4-6]. In response to estrogens, this plasma membrane localization favored the activation of protein kinase pathways (PI3K/Akt, Erk), endothelial nitric oxide (NO) synthase and phospholipase C [7-11], implicated in cell survival and migration. These rapid effects can also lead to gene expression changes[12, 13]. The physiological role of these membrane-initiated ERα actions *in vivo* began to be elucidated recently with the generation of the mouse model mutated for the palmitoylation site of ERα (*C451A-ERα*), demonstrating the importance of membrane actions for the fertility but also for some rapid vascular effects of E2, such as acceleration of reendothelialization and endothelial NO synthase phosphorylation and activation [14]. Finally, two pharmacological tools, the estrogen-dendrimer conjugate (EDC) and "pathway preferential estrogens" (PaPEs), showed that activation of MISS is sufficient to elicit these rapid endothelial effects [15-17].

While palmitoylation of ERα was found to be critical for its membrane targeting, a sequence in the C-domain of human ERα (aa251-260) [18] was also reported to allow the segregation between non-nuclear and nuclear actions of E2 [19]. Indeed, this motif was shown to interact with Gαi and be involved in rapid NO production in transfected COS cells. Interestingly, some point mutations within this domain, such as R256A, K257, D258A and R260A all abrogated the activation of eNOS and ERK phosphorylation in response to E2. By contrast, the E2-induced transcriptional response on ERE, SP1 and AP1-Luc gene reporter assays remained totally preserved, with the exception of R260A that abolished the response in an AP1 reporter gene assay. Furthermore, Le Romancer and coll. [20] demonstrated that the same arginine 260 residue was transiently methylated by PRMT1 following E2 activation, and that this methylation was required to trigger ERα interaction with the p85 subunit of PI3K and Src. The complex ERα/PI3K/src was found to be overexpress in a subset of breast tumors and is an independent marker of poor prognosis [21]. Nevertheless, the specific roles of this arginine 260 of ERα remained to be determined *in vivo*.

To that end, a knock-in mouse model of ERα mutated for the arginine 264 (the mouse counterpart of human arginine 260) into alanine was generated by homologous recombination (designated R264A-ERα). In contrast to several other mouse models mutated for ERα, the *R264A* female mice are totally fertile, with normal hormonal serum levels and a normal uterine and ovarian morphology. However, the rapid vascular effects of estrogens recognized to be initiated at the plasma membrane, such as rapid endothelial repair, eNOS activation and dilatation of arteries were lost in R264-ERα mice.

Material and Methods

Mice. All procedures were performed in accordance with the principles established by the INSERM and were approved by the local Ethical Committee of Animal Care N° CEEA-122-2014-55 and CEEA PdL 2012.105 for dilation and arterial remodeling. The *R264A-ERα* knock-in mouse line was generated on a C57BL6/N background at the Mouse Clinical Institute (Illkirch, France) by homologous recombination, as described in Supplementary Fig1. *R264A-ERα* and their corresponding wild-type littermates were ovariectomized at 4 weeks of age. For acute E2 treatment, they were subcutaneously (s.c.) injected with vehicle (castor oil) or 17β-estradiol (E2, 8 µg/kg) 3 weeks after ovariectomy. For chronic E2 treatment, ovariectomized mice were aleatory randomized to be implanted with s.c. pellets releasing either vehicle or E2 (8 or 80 µg/kg/day as indicated, 60-days release; Innovative Research of America, Florida).

Evaluation of estrous cycle. Estrous cycle was determined by vaginal cytology method [22] in 3 month-old adult mice for 10-20 consecutive days. Briefly, every morning, vaginal enema was performed with 20µL of Phosphate-buffered saline and cytology was determined by microscopic observations: predominant nucleate epithelial cells characterize proestrus phase; predominant corneous anucleate epithelial cells characterize estrus phase; leucocytes, as well as mix of nucleate and corneous anucleate epithelial cells characterize metestrus and diestrus phase.

Histological evaluation of ovarian function. Ovaries were dissected, fixed in 10% neutral buffered formalin for 24h, processed and embedded in paraffin. Slides were prepared by using transverse 4µm sections, deparaffinized and then stained by hematoxylin and eosin as previously described [23].

Immunohistochemistry:
Paraffin-embedded transverse sections (4 µm) from formalin-fixed uterine were stained as previously described [23] with anti–Ki67 (RM-9106; Thermo-scientific, culture supernatant, dilution 1/200), or with anti-ERα (MC-20, 50 ng/ml, Santa Cruz). Sections were examined after digitization using a NanoZoomer Digital Pathology®. To examine the proliferative effects of each treatment, the ratio of Ki67–positive epithelial cell/total cell number from two microscopic fields of measurement at x20 magnification for each uterine section was evaluated.

Hormone serums levels measurements. Serum levels of luteinizing hormone (LH) and follicle-stimulating hormone (FSH) were determined using the Multiplex Immunoassay Technology Xmap (MILLIPLEX, Millipore, St Quentin en Yvelines, France). Testosterone, Progesterone and 17β-estradiol were measured on serum of intact 10-12 week-old female mice using a gas chromatography-tandem mass spectrometry (GC-MS/MS) method as recently described [24].

Analysis of mRNA levels by RT-qPCR. Tissues were homogenized using a Precellys tissue homogenizer (Bertin Technol., Cedex, France), and total RNA from tissues was prepared using TRIzol (Invitrogen, Carlsbad, CA). RNA (0.5-1.0 µg) was reverse transcribed (RT) at 25°C for 10 min and then at 37°C for 2 h in 20 µL final volume using the High Capacity cDNA reverse transcriptase kit (Applied Biosystems). qPCR was performed on the equivalent of 7.5-20 ng of template using SsoFast EvaGreen Supermix (Bio-Rad) with primers validated for PCR efficiency and melt curve analysis (Supplementary Table 1). Results were normalized against the gene encoding the tumor protein, translationally-controlled 1 (*Tpt1*) (aorta) or *Gapdh/Hprt1* (uterus) using the geometric mean of relative quantities[25]. The data shown are geometrical means of relative quantities ($2^{-\Delta\Delta Cq}$ +/- linearized log2-based SEM) n=4/group) [26].

Micro-array. Total RNA was extracted using TriPure reagent (Roche, Lyon, France). Microarray data were obtained from 200 ng of uterine total RNA labeled with Cy3 using Low Input Quickamp Labeling Kit (Agilent, Massy, France) and hybridized to Agilent SurePrint G3 Mouse GE (8X60K) following the manufacturer's instructions. All experimental details and data are available in the Gene Expression Omnibus (GEO) database under accession GSE152344 . Data were analyzed with the LIMMA package in R (R 2.13., www.R-project.org). Hierarchical clustering was applied to the samples and the probes using 1-Pearson correlation coefficient as distance and the Ward's criterion for agglomeration. Functional analysis was carried out using DAVID Bioinformatics Resources 6.7 (http://david.abcc.ncifcrf.gov), and comparisons are realized with Venn Diagrams plug-in based upon the Venny tool developed by J.C Oliveros (GenoToul Bioinfo, Toulouse).

Integration of ChIP-seq data. We used the ER ChIP-seq data obtained from cultured cells of uteri (GSE36455) available at the GEO website [27]. Reads were aligned onto the indexed chromosomes of the mm9 genome using bowtie 0.12.7 [28] with parameters allowing at most two mismatches, and selected for unique mapping onto the genome. Peak calling was next performed as previously described [29] using samtools 0.1.12a [30] and MACS 1.4.1 [31] with default parameters. Identification of ERBss located at the vicinity of genes sub-populations and on genes TSSs used home-written intersection scripts and algorithms from the cistrome web-platform (http://cistrome.org/ap/;[32]). Motif analysis was performed using SeqPos tool on the cistrome web-platform. Motifs were declared enriched when *p*-values were <0.05 and Z-score>2.

Mouse carotid artery injury. Perivascular carotid artery electric injury was performed as previously described [14, 33, 34] on ovariectomized mice treated or not for 2 weeks before surgery with E2 (80 µg/kg/day in 60 day-release pellets). Briefly, the left common carotid artery was exposed via an anterior cervicotomy. The electric injury was applied to the distal part (3 mm precisely) of the common carotid artery with a bipolar microregulator. The percentage of reendothelialization was calculated relative to the initial de-endothelialized area by assessing Evans blue dye uptake 3 days after injury. Images were acquired under a DMR 300 Leica microscope, using Leica Application Suite V3.8 and ImageJ softwares.

Vascular reactivity of isolated mesenteric arteries. As previously described[35, 36], five-mm long segments of second-order mesenteric arteries from both male and female mice were dissected and mounted between 2 glass cannulae and bathed in a physiological salt solution (pH 7.4, pO2 160 mm Hg, and pCO2 37 mm Hg). Pressure was controlled by a servo-perfusion system, and diameter changes were measured continuously using a video-monitored system (Living Systems Instruments). Artery viability was assessed using KCl (80 mM) and endothelium integrity with acetylcholine (1 µM)-dependent dilation after precontraction with phenylephrine to approximately 50% of the maximal contractile response (Supplementary Figures 3A and 3B). E2-dependent dilation (0.01-1 µM) was then assessed after precontraction with phenylephrine to approximately 50% of the maximal contractile response obtained with KCl (80 mM). E2-dependent dilatation was repeated after treatment of the arterial segments with the NO synthesis blocker N-omega-Nitro-L-arginine (L-NNA, 0.1 mM). In a separate series of experiments, segments of second-order mesenteric arteries were mounted in an arteriograph as described above and incubated with pertussis toxin (200 ng/ml) for 2 hours. E2-dependent dilation (0.01-1 µM) was then tested after precontraction with phenylephrine to 70%.

Analyses of Atheromatous Lesions. Since sex differences have been frequently reported in mouse atherosclerosis studies[37] with a most widely reported sex effect on atherosclerosis in female mice, the E2 protective effect on atherosclerosis was only studied here in female mice, using the guidelines for experimental atherosclerosis studies described in the AHA

Statement [38]. Bilateral ovariectomy was performed, as previously described [14]. Two weeks after surgery, mice were switched to a hypercholesterolemic-atherogenic diet (1.25% cholesterol, 6% fat, no cholate; TD96335; Harlan Teklad, Madison, WI) and concomitantly received long-term estrogenic treatments. Mice were implanted with subcutaneous pellets releasing either placebo or 17β-estradiol (60-day release, 0.1 mg [ie, 80 µg/kg per day]) at weeks 6 and 12.
At the end of the protocol, overnight fasted mice were anesthetized with a combination of ketamine hydrochloride (100 mg/kg; Panpharma) and xylazine (5 mg/kg; Sigma-Aldrich) via intraperitoneal injection, and blood was collected from retro-orbital venous plexus. After euthanasia, the heart, the thoracic aorta, the liver, and the uterus were carefully dissected. Lipid deposition size was estimated at the aortic sinus, as previously described [33]. Briefly, each heart was frozen on a cryostat mount with optimal cutting temperature compound. One hundred 10-µm-thick sections were prepared from the top of the left ventricle, where the aortic valves were first visible, up to a position in the aorta where the valve cusps were just disappearing from the field. After drying for 2 hours, the sections were stained with oil red O and counterstained with Mayer's hematoxylin. One 10 µm-thick cut-section was collected from each 100 µm-thick zone was used for specific morphometric evaluation of intimal lesions using a computerized Biocom morphometry system. The first and most proximal section to the heart was taken 90 µm distal to the point where the aorta first becomes rounded. The mean lesion size (expressed in µm2) in these 10 sections was used to evaluate the lesion size of each animal.

Determination of Plasma Lipids. Overnight fasted mice were anesthetized, and blood samples were collected from the retro-orbital venous plexus. Total plasma cholesterol was assayed using the CHOD-PAD kit (Horiba ABX, Montpellier, France). The high-density lipoprotein fraction was isolated from 10 µl of serum and assayed using the "C-HDL+Third generation" kit (Roche, Lyon, France).

Blood Flow–Mediated Arterial Remodeling. Increase in blood flow, applied to the mesenteric artery, was performed, as previously described, on 4- to 5-month-old female mice [39]. Briefly, 3 consecutive first-order mesenteric arteries were used, and surgery consisted of ligatures of second-order branches. The artery located between the 2 ligated arteries was designated as the high-flow artery. Arteries located at a distance of the ligated arteries were used as controls (normal flow). After 14 days, mice were euthanized and mesenteric arteries were collected. Arteries were cannulated in an arteriograph as described above (vascular reactivity) and bathed in a Ca2+-free physiological salt solution containing ethylene-bis-(oxyethylenenitrolo) tetra-acetic acid (EGTA, 2 mmol/L) and sodium nitroprusside (SNP, 10 µmol/L). Pressure steps (10 to 125 mmHg) were then performed in order to determine passive arterial diameter. In each protocol, animals were anesthetized with isoflurane (2.5%). They were treated with buprenorphine (Temgesic; 0.1 mg/kg, SC) before and after surgery..

Western-blotting.
Mouse endothelial cells were isolated from aorta of wild-type and R264A-ERα mice, as previously described [40]. These mouse endothelial cells obtained from primary cultures and fresh tissues from uteri or testis were homogenized on Cell Lysis Buffer (TRis 80mM, pH=8; 5% SDS, 10% Glycerol) using a Precellys 24 (Bertin, France) with beads for the tissues. Total proteins (50 µg for testis and 10µg for uteri, all lysate for murine endothelial cells) were separated on Criterion TGX Stain-Free precast polyacrylamide 4-20% gels (Biorad) and transferred to nitrocellulose membranes using Trans Blot Turbo RTA Transfer Kit Midi 0.2µm Nitrocellulose. The following primary antibodies were used: anti-ERα (60C, 04-820, Millipore, culture supernatant, dilution 1/2000) and anti-β-actin (#BA3R, at 0.5 µg/ml, Arigo Biolaboratories) (Supplementary Table 2). Bands were revealed using HRP-conjugated secondary antibodies and visualized through ECL Prime detection, according to the manufacturer's instructions (GE Healthcare), using a ChemiDoc Imaging System (Bio-Rad). Bands were quantified using densitometry in the ImageJ software.

Statistical analyses. Results are expressed as the mean ± SEM. To test the effect of treatments or genotypes, Mann –Whitney test or unpaired t-test with Welch's correction were performed, as specified. To test the interaction between treatments and genotypes, a 2-way ANOVA was carried out. When an interaction was observed between two variables, the effect of treatment was studied in each genotype using the Bonferroni post hoc test. A value of $P<0.05$ was considered as statistically significant (*: $P<0.05$; **: $P<0.01$; ***: $P<0.001$).

Results

R264A mice are fertile and present a normal reproductive profile.

To study the potential role of arginine 264 of ERα in the rapid signaling *in vivo*, a knock-in strategy was employed in which the arginine 264, the murine counterpart of the human arginine 260, was mutated into alanine using a targeting construct containing two base-pair changes in exon 5 (Figure 1A and Supplementary Figures S1A and S1B). The R264A mutation was confirmed by PCR using tail DNA as template (Supplementary Figure S1C). Since the fertility is usually altered in mice mutated for ERα, including the mice mutated specifically for the palmitoylation site [14], the reproductive capacity of R264A mice was first evaluated. The *R264A-ERα* female mice were found totally fertile when continuously mated with wild type males (0.8 litters/month/female; 6.5 pups/litter) as compared to WT mice (0.6 litters/month/female; 6.5 pups/litter). To further evaluate the ovarian function, estrous cyclicity was then evaluated by daily vaginal cytology (Figure 1B). As illustrated in Figure 1B, *R264A-ERα* females alternated proestrus, estrus, met/diestrus phases in a similar way than WT mice with regular estrous cycles. Histomorphological analysis of the ovaries showed normal structure, with in particular many corpus luteum and absence of any cystic or hemorrhagic follicles (Figure 1C). Uteri were also normal on their gross appearance and the uterine weights of WT and *R264A-ERα* mice remained similar (Figures 2A and 2B). As an initial characterization of this mouse model, we also evaluated the expression of ERα protein in uterus from littermate wildtype (WT-ERα) and mutant R264A-ERα mice. ERα protein abundance detected by western blot in the uterus was similar in the two groups (Figures 2C-D). Moreover, immunodetection of ERα in uterus clearly detect ERα on uterine epithelial and stromal cells without any difference between nuclear and extra-nuclear staining between the 2 genotypes (Figure 2E). Serum levels of gonadotropin and ovarian sexual hormones were finally measured in intact 10-12 week old female mice (Table 1). All these hormones were present in similar levels in the serum of *R264A-ERα* mice as compared to their WT littermates.

Altogether, these data demonstrate that the *R264A-ERα* mice are fertile with no detectable perturbation of the hypothalamic-pituitary-ovary axis and steroidogenesis.

Nuclear actions of *R264A-ERα* are widely conserved in the uterus

Previous studies performed *in vitro* in transfected HeLa cells have shown that this specific human counterpart mutant ERα-R260A displays normal capacity to activate gene transcription via direct ERE-mediated binding to DNA as well as indirect, tethered, DNA binding via the transcription factors Sp1. In contrast, AP-1-mediated transcriptional transactivation was not activated by E2 binding to this ERα-R260A [19]. Furthermore, O'Brien et al. (2006) [41] suggested that this non-ERE transcriptional response impacted the estrogen-induced proliferation of uterine epithelial cells. We therefore studied the uterotrophic response to E2 by comparing uterine wet weights in ovariectomized female mice 24 hours after a single subcutaneous injection of vehicle or 8µg/kg of E2 . Acute E2 treatment caused a slightly but significantly greater increase in uterine weight in *R264A-ERα* as compared to WT-ERα mice. Ki-67 labeling was also performed 24h following E2 (Figure 2F). A slightly but significant increased epithelial proliferation was also observed in R264-ERα mice as compared to WT mice (92.9±1.7 for *R264A-ERα* as compared to 76.9± 7.6 for *WT*, Inter. $P=0.0375$; Gen $P=0.039$; E2 $P<0.0001$) (Figures 2G-H).

Despite similar uterine weights observed in intact 3-months old female mice, the differences in uterine weights and epithelial proliferation observed in acute experiments (Figures 2F and 2H) led us to extensively evaluate the capacity of R264A-ERα to activate gene transcription *in vivo* in uteri 6 hours after acute s.c. E2 treatment (8µg/Kg). The E2-regulated genes in *R264A-ERα* and WT mice as compared to placebo is presented in the volcano plot in Figure 3A ($P<0.05$). Cluster analysis of all of the tested conditions identified two major patterns of gene expression corresponding to genes down- or up- regulated genes by E2 (Figure 3B). The patterns of genes regulated by E2 by the R264A mutant are very similar to control WT littermates treated by E2. Importantly, 15,409 probes are regulated by E2 treatment in WT mice, which is almost identical to the 15,247 E2-regulated genes in R264A mice (absolute Fold change >1.5; P value <0.05). In terms of fully Ensembl annotated genes, the Venn-diagram in Figure 3C indicates that 7,283 genes are commonly regulated genes from totals of 8,102 and 8,039 genes regulated by E2 in WT or R264A mice, respectively. By consequence, only a small number of genes were regulated in an ERα-R264A dependent manner: 756 genes (around 8.5% of total regulated genes) as compared to 819 genes regulated in an ERα-WT dependent manner (9.2% of total regulated genes). However, only 3 probes were significantly differentially regulated by E2 between the 2 genotypes, corresponding to *Gpsm2, Il11 and Fam178b* (Figure 3B). At a lower stringency, one other gene, *Kalrn* was also declared as being differentially expressed. Since the number of differentially dysregulated genes by E2 was so low between WT and R264A, we reanalyzed these data by performing the BH correction on *P*-values after the selection of probes on their expression (*P*val2 in the Table provided within Figure 3D). This procedure similarly identified *Fam178b* and *Il-11* as well as *Kalrn* with a lower stringency. From this total of 6 genes, statistical differences between WT and R264A-ERα gene expression for 4 of these genes, i.e *Gpsm2, Nmur2, Kalrn and IL11* were validated by RT-qPCR (Figure 3E). The *Gpsm2* (G-protein signaling modulator 2) and *Nmur2* (encoding a protein for the Neuromedin U receptor, which is part of a G-protein coupled receptor 1 family) were less expressed in the uteri from E2-treated *R264A-ERα* mice as compared to WT (fold change -1.5 and 2, respectively). By contrast, the *Il11* (interleukin 11) is highly induced in response to E2, and 2-fold more induced in *R264A-ERα* mice as compared to WT mice, while the Kalrn (encoding a Kalirin RhoGEF Kinase) is more highly induced by E2 in *R264A-ERα* as compared to the WT.

While AP1-mediated transcriptional activation by E2 has been reported to be deficient in HeLa cells transfected with the human counterpart of R264A (i.e. R260A) [19], we thus aimed at determining whether this observation could translate into the fact that, despite a very low number of differentially regulated genes between the 2 genotypes. 819 and 756 genes were identified as specifically E2-regulated genes in either *WT* or *R264A* mice respectively. We took advantage of the published ERα cistrome (entirety of ER binding events on chromatin) in uterine *WT* cells[27] to assess whether these WT or R264A- specific E2 regulated genes were at the vicinity or not of these ERBSs (Estrogen Receptor Binding Sites). Similar number of ERBs in a 10 kb window centered at their Transcription start site (TSS) were found in genes regulated in WT or R26AA conditions (Supplementary Figures S2A-C and Table S2) while analysis of the transcription factor motifs included within the ERBSs found at the proximity of these genes indicate that AP1 (ATF2/Jun heterodimers TFs) motifs are absent from the ERBSs located at the vicinity of genes specifically regulated by E2 in *R264A-ERα* mice only.

Taken together, considering that only 4 genes were differentially regulated by E2 between *R264A-ERα* and its wild type littermates as compared to the 8,000 genes on average regulated by E2 in both genotypes, we conclude that R264A has minor impact on gene expression regulation in the uterus in response to E2.

Membrane-initiated vascular actions of ERα, such as acute E2-induced dilation are abrogated in *R264A-ERα* mice.

Non-genomic actions of estrogens has been found to be particularly implicated in some protective vascular effects of E2, i.e. rapid dilatation and acceleration of re-endothelialization [14-17]. So, we first evaluated whether expression of ERα protein level was conserved in primary culture of endothelial cells of WT and R264-ERα mice. As shown in Figures 4A-B, R264A-ERα protein abundance was similar to WT-ERα. We then evaluated the acute dilation following addition of ~~stepwise doses~~E2 (0.01-1 µM) in WT and R264A mesenteric arteries from female mice, after precontraction with phenylephrine. Typical tracings of the results are shown in Figure 4C. We first checked that the KCl-mediated contraction of the arteries and the precontraction level of the arteries before E2-mediated dilation were similar between the two genotypes (Supplementary Figures 3A-B). In female WT mice, E2 induced a concentration-dependent dilation, which was significant at an E2 concentrations of 10^{-7} M (20.3± 4.3%) and 10^{-6} M (40.7± 3.7%) compared to vehicle-treated WT vessels (8.6± 3.6% and 10.3± 3.6%, respectively) (Figure 4D). A significant effect of E2 was found in the WT-ERα at 10^{-7} and 10^{-6} (* (*P*<0.05) and *** (*P*<0.001) respectively), while E2-induced dilatation was completely absent in *R264A-ERα* arteries treated with 10^{-6} M E2 (13.0 ± 2.2% compared to vehicle: 10.3 ± 2.2%). L-NNA, an inhibitor of NO synthesis, blocked E2-induced dilation of WT arteries (-0.5 ± 3.6%) (Figure 4E), but had any additional inhibitory effect on the unresponsive R264-ERα arteries to E2 (8.1 ± 6.0%). The L-NNA inhibitory effect on the E2-mediated dilation of mesenteric arteries suggested that these rapid membrane effects of estrogens are essentially mediated through the rapid stimulation of eNOS-dependent production of NO as previously shown in the human coronary artery [42].The L-NNA inhibitor effect of e-NOS was also tested on acetylcholine-induced dilation of WT and R264A-ERα mice (Figure 4F) to confirm that the NO signaling is operating properly in the R264A-ERα while it is only altered by the arginine mutation in response to E2. Sex differences in the E2-induced acute dilation of mesenteric arteries were then tested, using mesenteric arteries from male mice. Typical tracings and results (Supplementary Figure 4) totally matched results obtained in female mice, with a significant E2-induced acute dilation in male WT arteries (40.3± 4.8 % with E2 10^{-6} M) and an absence of dilation in R264A-ERα mice in response to E2 10^{-6} M (12.9± 2.6 %) as compared to WT-EtOH and R264-ERα-EtOH (18.3± 9 % and 18.6± 4.1, respectively). Fertility of these male mice was also totally normal, with no impact of the R264A-ERα mutation on the reproductive tissues (Supplementary Figure 5). Previous studies performed in both an immortalized endothelial cell line and in transfected COS cells have shown that the C-domain of human ERα (aa251-260) was required to interact with Gαi and be involved in rapid NO production[43]. To further investigate the importance of R264A-ERα in this interaction and in this E2-acute induced dilation, mesenteric arteries from female WT-ERα mice were pretreated with pertussis toxin (PTX) for 120 min and further stimulated with E2. Figure 4G indicates that this pre-treatment with PTX totally abrogated the rapid E2-induced dilation, revealing the important role of R264A-ERα in the interaction with G proteins.

Membrane-initiated vascular actions of ERα, such as acceleration of re-endothelialization after electric carotid injury are abrogated in *R264A-ERα* mice.

The role of R264 was then investigated *in vivo* by evaluating re-endothelialization of the carotid artery after electric injury in response to E2, an effect previously demonstrated to be exclusive membrane ERα effects [14, 15, 17] (Figure 5A). As observed on the photographs of the Evans Blue staining and on the corresponding quantifications of re-endothelialization, E2 treatment caused 2-fold increase in endothelial repair in WT mice (37.6 ± 3.3 % and 19.4 ± 2.7 % in WT mice treated or not with E2, respectively), whereas it had no effect in *R264A-ERα* mice (21.1 ± 1.9 % as compared to 17.7 ± 2.4 %). We previously demonstrated that this E2 action required ERα in both the endothelial and hematopoietic cells [34]. To further explore the role of hematopoietic cells ERα in this process, WT mice were irradiated and grafted with either WT or *R264A-ERα* bone marrow (Figure 5B). The E2 effect was still present in WT mice grafted whatever the genotype, indicating that the non-genomic actions of ERα in the bone marrow are not required for the accelerative effect of E2, suggesting a role for the non-

genomic effects of ERα in the vasculature rather than in the hematopoietic cells for the acceleration of re-endothelialization.

Altogether these results demonstrate that arginine 264 is crucial for the membrane initiated endothelial effects of ERα, namely vascular dilatation and acceleration of re-endothelialization in response to E2.

Effect of E2 on atheroma and flow-mediated remodeling in *R264A-ERα* mice.

Estrogens have numerous well-known protective vascular effects, besides their effects on re-endothelialization and arterial remodeling. E2 is, in particular, involved in the prevention of atheroma and in flow-mediated remodeling that are known to involved nuclear actions of estrogens[44]. We first analyzed the nuclear response of E2 in aorta, by comparing gene expression profile in the aorta from *R264A-ERα* with their littermate WT controls, 6 hours after acute E2 administration. As illustrated in Figure 6A, all genes tested were similarly regulated in both genotypes as revealed by absence of interaction between genotype and treatment after 2-way ANOVA analysis for all the genes analyzed, neither for up-regulated genes (*Grem2, Gatnl2, Myc, Cam2kb, Tiparp*) nor the down-regulated ones (*Shisha*2).

We then investigated the impact of the R264A-ERα mutation on arteries submitted to an atherogenic stress. Our previous works demonstrated that atheroprotection is entirely dependent on nuclear ERα[45]. To this aim, *R264A-ERα* mice were bred with *LDLr*$^{-/-}$ mice and fed an hypercholesterolemic diet for 12 weeks. E2 treatment similarly decreased fatty streak deposits at the aortic sinus of both *LDLr* $^{-/-}$ and *R264A- ERα/LDLr*$^{-/-}$ mice (Figures 6B and 6C). We also assessed the role of R264A-ERα in the lipid profile (Table 2). As previously described [33], both plasma cholesterol and HDL cholesterol fractions were decreased by E2 and these effects were similarly observed in *R264A-ERα* mice. As expected, ovariectomy led to uterine atrophy. Exogenous E2 replacement induced uterine hypertrophy in both *R264A-ERα/LDLr*$^{-/-}$ and their littermate controls, with body weights being similar whatever the genotype (Table 2).

Finally, we investigated flow-mediated remodeling of resistance arteries from *R264A-ERα* mice and their wild type littermates. Two weeks after adjacent arterial ligation *in vivo*, arterial diameter was determined *in vitro* in response to stepwise increases in intraluminal pressure (Figures 6D and 6E). The increase in passive arterial diameter in response to increases in pressure was significant and similar in high-flow arteries from WT mice, and from *R264-ERα* mice.

Altogether, these results demonstrated that R264 is not necessary to mediate these two vascular effects of E2, recognized as being dependent on nuclear, but not MISS, ERα actions[44], segregating the nuclear/membrane vascular effects of E2.

Discussion

In the present study, we used the *R264A-ERα* mice to determine whether the point mutation of arginine 264 into alanine into murine ERα affects the physiological functions of this steroid receptor *in vivo*. Our findings reveal that the amino acid R264 is not crucial neither for female or male fertilities nor for ERα-regulated gene expression regulation in aorta and uterus. In contrast, R264 is selectively required for the vascular membrane initiated actions of ERα. Indeed, *R264A* mice presented an absence of E2-induced acceleration of re-endothelialization and rapid NO-induced vasodilatation while it is dispensable for prevention of atherosclerosis and arterial remodeling. Thus, *R264A* mouse is the first model without any endocrine and reproductive alteration that genetically segregates nuclear and membrane effects of ERα in the vasculature.

We have first determined the reproductive phenotype of female *R264A* mice, looking at the estrous cycle, the ovarian function and quantifying the sexual hormone levels. *R264A-ERα* mice are totally fertile with regular estrous cycle profiles. The ovarian function is entirely preserved, as attested by the presence of corpus luteum which confirmed that ovulation has occurred. LH serum levels, which are typically affected in all previous ERα mutants, are

normal in *R264A-ERα* mice. Moreover, circulating ovarian hormones levels such as estradiol, progesterone and testosterone are completely normal as compared to WT mice, suggesting the absence of any deregulation of ERα functions in steroidogenesis and hypothalamic-pituitary-axis (HPO). This result is at first glance surprising, because all ERα mutant mice generated so far are infertile, including the previous mouse models C451A and NOER, mutated on the palmitoylation site C451 of ERα that abrogated the membrane effects of estrogens [46]. Indeed, the C451A mice presented polycystic and hemorrhagic ovaries and an increase in LH serum levels, clearly demonstrating the role of membrane ERα in fertility[14]. Nevertheless, only another mouse model reported as impaired for membrane ERα signaling remained fertile: the *DPM* mouse model, in which membrane ERα signaling is impeded by overexpression of a peptide that prevents ERα interaction with striatin [47]. Striatin directly binds to aa176-253 of ERα and serves as a scaffold protein to form and stabilize ERα caveolar complex with eNOS[48]. Overexpression of disrupted peptide corresponding to aa176-253 blocked ERα/Striatin interaction and prevented E2-induced MAPK, Akt and eNOS activation, but did not abolished ERE-dependent transcriptional activity *in vitro* [48]. Altogether C451A, DPM and *R264A-ERα* mice reveal the complexity of membrane ERα sub-signaling in the control of female fertility. Importantly, since deletion of aa250-274 has been demonstrated to do not disturb plasma membrane localization of ERα [49] contrary to the C451A mutation [4, 14], this discrepancy could explain their respective fertility profiles. *R264A-ERα* mice clearly demonstrate that the R264 residue and thus, as discussed below, ERα methylation and/or ERα/ $G\alpha_i$ interaction, are not crucial for the phenotype of female and male fertility.

We explored the transcriptional regulation ability of the mutated R264A-ERα. Previous *in vitro* studies have shown that R264A mutation did not alter ERE-dependent transcriptional regulation, but affected the indirect AP1-dependent regulation of transcription [19]. Using EDC to activate MISS effects or interrogating the mutant ERα-C451A *in vitro*, membrane initiated actions of estrogens were also reported to secondary modulate the nuclear transcriptional response *in vitro* [12, 13]. The large scale analysis performed on R264A uteri provided a broad overview of the E2 effect on gene transcription. Surprisingly, almost all gene transcriptional regulation by E2 is conserved in *R264A-ERα* mice as compared to *WT* mice. Even though E2 is a master regulator of gene transcription on the uterus (8800 differentially expressed genes), the R264A mutation has a minor impact on gene regulation (6 genes) as compared to the C451A mutation. Among these genes, it is interesting to note that the *Gspm2* which encodes a G protein signaling modulator is down-regulated by E2 in *R264A-ERα* as compared to WT. This protein is also called LGN (Leu-Gly-Asn repeat enriched protein) and it has been shown to modulate the activity of the NO receptor soluble guanylate cyclase[50], a major actor of the downstream NO signaling pathway. Among the 3 other validated genes by RT-qPCR, one is the *Il-11*, the interleukin-11, reflecting a potential impact on immunity while the Kalrn encodes a Kalirin RhoGEF Kinase. It is interesting to note that even though rare genes are found to be dysregulated by E2 between WT an *R264A-ERα*, two of these genes encodes signaling proteins (*Gpsm2* and *Kalrn*), probably pointing the importance of R264 on the rapid signaling pathway of ERα. As already mentioned in luciferase reporters assays in Hela cells [51], our motif analysis further indicated that AP1 binding sites may be absent from promoters and putative ER binding regions controlling the activity of the genes specific for the *R264A-ERα* mouse uteri. Whether this observation is actually true could be stressed by determining the cistrome of AP1 in both mouse genotypes. Physiologically, the mutation R264A induces a slight but significant increase in uterine weight and epithelial proliferation following acute E2 treatment without any impact on uterine weights in intact mice. This transient increase in uterine weight at 24 hours might be due to edema induced by impacted vascular effects of E2[52]. But, this small increase in proliferation could have consequences in tumor cells, since the R264 motif has been shown to be involved in activation of Akt in breast cancers [21]. However, the functional importance of this hypothetical change in the balance of ERα activity through indirect/direct binding in uteri caused by the R264A seems at the end very low in this tissue in physiological conditions, as most transcriptional regulations are unchanged.

In contrast to the uterus where 8800 genes are found regulated by E2, a large microarray analysis performed on the aorta of *DPM* mice has demonstrated that only 200 genes in average are regulated by E2 on WT mice following 4 hours treatment [47]. However, in *DPM* mice, the transcriptional response to E2 was greatly altered. These results suggested that ERα /Striatin interaction and thus membrane ERα signaling plays a major role in vascular gene regulatory response to estrogen. Nevertheless, the disrupting strategy by overexpression of blocking peptide may induce off-target effects, as indicated by authors, especially on ERβ. In this present work, the R264A mutation does not significantly altered the gene transcriptional response on any of the tested genes. Altogether, these results demonstrated that the R264A mutation does not alter significantly the transcriptional activity of ERα neither in uterus nor in aorta.

Nevertheless, in contrast to this preservation of gene expression by E2 in aorta from *R264A-ERα* mice, the membrane-initiated vascular actions of ERα are abrogated in *R264A-ERα* mice. Contrary to *WT* mice, *R264A-ERα* mice do not show any accelerative effects of E2 on re-endothelialization of carotid after electric injury. This E2 vascular effect is undoubtly the most characterized *in vivo* model of membrane ERα signaling of estrogens. Indeed, EDC (Estrogen Dendrimer conjugate), which only activates membrane ER, is sufficient to induce acceleration of re-endothelialization [15]. Furthermore, we recently demonstrated that this effect is lost in membrane *C451A-ERα* mutant mice, whereas it is conserved in both ERα mutant mice mutated for either the AF2 or the AF1 transactivation function [14]. In addition, the female *R264A-ERα* mice lost the E2-dependent vasodilatory response in mesenteric arteries, as previously observed in *C451A-ERα* mice. No sex difference was observed in this E2 vascular effect, since this rapid E2-induced dilation was also observed in WT males, but also lost in male R264A-ERα mice. Interestingly, this E2-induced acute dilation in mesenteric arteries was completely abrogated by an NO synthesis inhibitor (L-NNA), highlighting the crucial role of eNOS activity and NO production in these membrane initiated vascular effects of E2. This is in agreement with previous works by our group[44] and others (review of the literature in [17]). In contrast, previous data [53] have demonstrated that the presence of eNOS but not its enzymatic activity is determinant for estrogen signaling in the the endothelium for re-endothelialization. These studies concur to underline that, according to the model and the vascular function explored, membrane ERα may have different interactions and relationships involving either the eNOS activity or the presence of eNOS protein as a scaffolder. Our present data further demonstrate no involvement of R264-ERa signaling in the E2 atheroprotective effect and vascular remodeling even though this mutation abrogates NO-dependent rapid dilation. This result is consistent with the literature as the E2-induced atheroprotective effect was reported to be conserved after NOS inhibition [54] and in hypercholesterolemic eNOS$^{-/-}$ mice [55] even though the eNOS-KO mice have been reported to exhibit accelerated atherosclerosis. Altogether, these results highlight the complexity of E2/ERα/eNOS pathways depending of the experimental model used and the engagement of membrane versus nuclear ERα.

Therefore, it is clear that R264-ERα is crucial for two membrane-initiated vascular effects of E2, namely eNOS acute activation during E2-mediated dilation of mesenteric arteries and acceleration of endothelial healing.while it is dispensable for the prevention of atherosclerosis and arterial remodeling, known to be mediated by nuclear/genomic actions of E2, extending previous observations done with C451A-ER*α* mice, impeded for ERα membrane location [44]. More recently, G protein-coupled estrogen receptor 1 (GPER) has been proposed as a third Estrogen receptor present at the membrane and been reported to mediate some beneficial cardiovascular effects of estrogens, as endothelium-dependent and nitric oxide-dependent effects of E2 and prevention of atherosclerosis [56, 57]. GPER could concur to the protective action of E2, but nuclear ERα is absolutely required as this E2 action if lost in the AF2°-ERα mice [45].

Finally, a question remains open concerning the respective roles of ERα methylation and ERα/Gα_i interaction in the observed R264A phenotype. Indeed, R260 have been studied from two different points of view. On one hand, R260 has been seen as a methylation site

necessary for ERα/Src/PI3K complex formation in response to E2 that mediates the Akt induced proliferation of the epithelium [20]. On the other hand, Shaul and coll. have shown that R260 is also part of a domain interacting with $G\alpha_i$ and this ERα/Gαi interaction is further enhanced by E2 and necessary for eNOS activation [15, 20, 58]. The *in vivo* results on the microarray analysis revealed the down-regulation of a G protein modulator that is in agreement with the interaction with the Gαi protein. Moreover, pretreatment *in vitro* of mesenteric arteries with pertussis toxin abrogated the acute E2-induced dilation, highlighting the involvement of protein G activation in this E2-induced vasodilatory action which is lost in R264A-ERα mice. Wu and his collaborators [19] have previously shown that the aspartic acid D258A-ERα was unable to associate with Gi, preventing eNOS activation by E2. We further demonstrate here that the arginine 264 residue (counterpart of 260 in human ERα) is necessary and sufficient to mediate eNOS activation by E2, likely through interaction with G protein. A question remains open: is methylation of ERα in response to E2 involved in the conformational change of ERα implicated in the ERα /Gαi interaction? In that case, methylation of ERα could be a requirement for Gαi interaction that will further activate the downstream signaling. However, this model and kinetics of interaction are out of reach and beyond the scope of *in vivo* studies, in particular as this methylated form appeared very transient. In consequent, *in vitro* studies in appropriate models should be done to further understand the molecular mechanism(s) involved.

In conclusion, steroid receptors are capable to elicit rapid, nongenomic actions, but mouse models which allow to study the physiological role of these original actions so far called nuclear receptor remains limited to estrogen receptor. Indeed, after the palmitoylable C451 residue, the arginine 264 represents the second major amino acid absolutely necessary for membrane ERα signaling in the vasculature. In contrast, the transcriptional gene regulation by E2 is highly conserved in aorta and uterus of these mice, demonstrating that R264 is essentially dispensable for these gene expression changes and supporting the idea that MISS and nuclear actions are independent in the arteries. Finally, these findings support and extent the conclusions previously established with *AF2^0-ERα* and *C451A-ERα* mice[44], and will help to further delineate the medical potential of the selective activation/inhibition of MISS and nuclear ERα actions.

Acknowledgments

The staff of the animal facilities (in particular P. Espagnolle and G. Carcassès) and of the “Plateforme d’expérimentation fonctionnelle” is acknowledged for their skillful technical assistance. We also thank J. Guillermet and B. Masri for helpful discussions. We are also grateful to M. Garcia. and C. Proux (Angers) for their technical helps for experiments in E2-acute dilation, I. Bleuart and I. Pardo for providing excellent technical support and advice regarding the histology (ENVT). We are also grateful to Y. Lippi for its excellent contribution to the microarray analysis performed at the GeT-TQ Genopole Toulouse Facility and to Isabelle Bleuart and Isabelle Pardo for providing excellent technical support and advice regarding the histology (ENVT).

Sources of Funding

This work was also supported by the INSERM, the Université de Toulouse III, the Fondation pour la Recherche Médicale), The Région Midi-Pyrénées and FEDER (Fonds européen de développement régional (REGEN-EVE), the ANR (Agence Nationale de la Recherche, Estroshear, contract # ANR-18-CE14-0016-01), the CNRS, the University of Rennes1. M.A. was supported by grant from the Ministere de la Recherche. C.F was supported by ANR-18-CE14-0016-01.

Disclosures:

Nothing to disclose

All data and supporting materials have been provided with the published article

References

1. Heldring N, Pike A, Andersson S, Matthews J, Cheng G, Hartman J, Tujague M, Strom A, Treuter E, Warner M, Gustafsson JA. Estrogen receptors: How do they signal and what are their targets. *Physiological reviews*. 2007;87:905-931
2. Pietras RJ, Szego CM. Specific binding sites for oestrogen at the outer surfaces of isolated endometrial cells. *Nature*. 1977;265:69-72
3. Szego CM, Davis JS. Adenosine 3',5'-monophosphate in rat uterus: Acute elevation by estrogen. *Proceedings of the National Academy of Sciences of the United States of America*. 1967;58:1711-1718
4. Acconcia F, Ascenzi P, Bocedi A, Spisni E, Tomasi V, Trentalance A, Visca P, Marino M. Palmitoylation-dependent estrogen receptor alpha membrane localization: Regulation by 17beta-estradiol. *Mol Biol Cell*. 2005;16:231-237
5. Acconcia F, Ascenzi P, Fabozzi G, Visca P, Marino M. S-palmitoylation modulates human estrogen receptor-alpha functions. *Biochem Biophys Res Commun*. 2004;316:878-883
6. Pedram A, Razandi M, Sainson RC, Kim JK, Hughes CC, Levin ER. A conserved mechanism for steroid receptor translocation to the plasma membrane. *J Biol Chem*. 2007;282:22278-22288
7. Hammes SR, Levin ER. Minireview: Recent advances in extranuclear steroid receptor actions. *Endocrinology*. 2011;152:4489-4495
8. Kim KH, Bender JR. Membrane-initiated actions of estrogen on the endothelium. *Mol Cell Endocrinol*. 2009;308:3-8
9. Wu Q, Chambliss K, Umetani M, Mineo C, Shaul PW. Non-nuclear estrogen receptor signaling in the endothelium. *J Biol Chem*. 2011;286:14737-14743
10. Simoncini T, Genazzani AR. Non-genomic actions of sex steroid hormones. *Eur J Endocrinol*. 2003;148:281-292
11. Simoncini T, Hafezi-Moghadam A, Brazil DP, Ley K, Chin WW, Liao JK. Interaction of oestrogen receptor with the regulatory subunit of phosphatidylinositol-3-oh kinase. *Nature*. 2000;407:538-541
12. La Rosa P, Pesiri V, Leclercq G, Marino M, Acconcia F. Palmitoylation regulates 17beta-estradiol-induced estrogen receptor-alpha degradation and transcriptional activity. *Mol Endocrinol*. 2012;26:762-774
13. Madak-Erdogan Z, Kieser KJ, Kim SH, Komm B, Katzenellenbogen JA, Katzenellenbogen BS. Nuclear and extranuclear pathway inputs in the regulation of global gene expression by estrogen receptors. *Mol Endocrinol*. 2008;22:2116-2127
14. Adlanmerini M, Solinhac R, Abot A, Fabre A, Raymond-Letron I, Guihot AL, Boudou F, Sautier L, Vessieres E, Kim SH, Liere P, Fontaine C, Krust A, Chambon P, Katzenellenbogen JA, Gourdy P, Shaul PW, Henrion D, Arnal JF, Lenfant F. Mutation of the palmitoylation site of estrogen receptor alpha in vivo reveals tissue-specific roles for membrane versus nuclear actions. *Proceedings of the National Academy of Sciences of the United States of America*. 2014;111:E283-290
15. Chambliss KL, Wu Q, Oltmann S, Konaniah ES, Umetani M, Korach KS, Thomas GD, Mineo C, Yuhanna IS, Kim SH, Madak-Erdogan Z, Maggi A, Dineen SP, Roland CL, Hui DY, Brekken RA, Katzenellenbogen JA, Katzenellenbogen BS, Shaul PW. Non-nuclear estrogen receptor alpha signaling promotes cardiovascular protection but not uterine or breast cancer growth in mice. *The Journal of clinical investigation*. 2010;120:2319-2330
16. Madak-Erdogan Z, Kim SH, Gong P, Zhao YC, Zhang H, Chambliss KL, Carlson KE, Mayne CG, Shaul PW, Korach KS, Katzenellenbogen JA, Katzenellenbogen BS. Design of pathway preferential estrogens that provide beneficial metabolic and vascular effects without stimulating reproductive tissues. *Sci Signal*. 2016;9:ra53
17. Arnal JF, Lenfant F, Metivier R, Flouriot G, Henrion D, Adlanmerini M, Fontaine C, Gourdy P, Chambon P, Katzenellenbogen B, Katzenellenbogen J. Membrane and nuclear estrogen receptor alpha actions: From tissue specificity to medical implications. *Physiological reviews*. 2017;97:1045-1087
18. Krust A, Green S, Argos P, Kumar V, Walter P, Bornert JM, Chambon P. The chicken oestrogen receptor sequence: Homology with v-erba and the human oestrogen and glucocorticoid receptors. *The EMBO journal*. 1986;5:891-897
19. Wu Q, Chambliss K, Lee WR, Yuhanna IS, Mineo C, Shaul PW. Point mutations in the eralpha galphai binding domain segregate nonnuclear from nuclear receptor function. *Mol Endocrinol*. 2013;27:2-11

20. Le Romancer M, Treilleux I, Leconte N, Robin-Lespinasse Y, Sentis S, Bouchekioua-Bouzaghou K, Goddard S, Gobert-Gosse S, Corbo L. Regulation of estrogen rapid signaling through arginine methylation by prmt1. *Molecular cell*. 2008;31:212-221
21. Poulard C, Treilleux I, Lavergne E, Bouchekioua-Bouzaghou K, Goddard-Leon S, Chabaud S, Tredan O, Corbo L, Le Romancer M. Activation of rapid oestrogen signalling in aggressive human breast cancers. *EMBO Mol Med*. 2012;4:1200-1213
22. Caligioni CS. Assessing reproductive status/stages in mice. *Current protocols in neuroscience*. 2009;Appendix 4:Appendix 4I
23. Abot A, Fontaine C, Raymond-Letron I, Flouriot G, Adlanmerini M, Buscato M, Otto C, Berges H, Laurell H, Gourdy P, Lenfant F, Arnal JF. The af-1 activation function of estrogen receptor alpha is necessary and sufficient for uterine epithelial cell proliferation in vivo. *Endocrinology*. 2013;154:2222-2233
24. Nilsson ME, Vandenput L, Tivesten A, Norlen AK, Lagerquist MK, Windahl SH, Borjesson AE, Farman HH, Poutanen M, Benrick A, Maliqueo M, Stener-Victorin E, Ryberg H, Ohlsson C. Measurement of a comprehensive sex steroid profile in rodent serum by high-sensitive gas chromatography-tandem mass spectrometry. *Endocrinology*. 2015;156:2492-2502
25. Vandesompele J, De Preter K, Pattyn F, Poppe B, Van Roy N, De Paepe A, Speleman F. Accurate normalization of real-time quantitative rt-pcr data by geometric averaging of multiple internal control genes. *Genome Biol*. 2002;3:RESEARCH0034
26. Taylor SC, Nadeau K, Abbasi M, Lachance C, Nguyen M, Fenrich J. The ultimate qpcr experiment: Producing publication quality, reproducible data the first time. *Trends Biotechnol*. 2019;37:761-774
27. Hewitt SC, Li L, Grimm SA, Chen Y, Liu L, Li Y, Bushel PR, Fargo D, Korach KS. Research resource: Whole-genome estrogen receptor alpha binding in mouse uterine tissue revealed by chip-seq. *Mol Endocrinol*. 2012;26:887-898
28. Li H, Handsaker B, Wysoker A, Fennell T, Ruan J, Homer N, Marth G, Abecasis G, Durbin R, Genome Project Data Processing S. The sequence alignment/map format and samtools. *Bioinformatics*. 2009;25:2078-2079
29. Palierne G, Fabre A, Solinhac R, Le Peron C, Avner S, Lenfant F, Fontaine C, Salbert G, Flouriot G, Arnal JF, Metivier R. Changes in gene expression and estrogen receptor cistrome in mouse liver upon acute e2 treatment. *Mol Endocrinol*. 2016;30:709-732
30. Langmead B, Trapnell C, Pop M, Salzberg SL. Ultrafast and memory-efficient alignment of short DNA sequences to the human genome. *Genome biology*. 2009;10:R25
31. Zhang Y, Liu T, Meyer CA, Eeckhoute J, Johnson DS, Bernstein BE, Nusbaum C, Myers RM, Brown M, Li W, Liu XS. Model-based analysis of chip-seq (macs). *Genome biology*. 2008;9:R137
32. Liu T, Ortiz JA, Taing L, Meyer CA, Lee B, Zhang Y, Shin H, Wong SS, Ma J, Lei Y, Pape UJ, Poidinger M, Chen Y, Yeung K, Brown M, Turpaz Y, Liu XS. Cistrome: An integrative platform for transcriptional regulation studies. *Genome biology*. 2011;12:R83
33. Billon-Gales A, Fontaine C, Filipe C, Douin-Echinard V, Fouque MJ, Flouriot G, Gourdy P, Lenfant F, Laurell H, Krust A, Chambon P, Arnal JF. The transactivating function 1 of estrogen receptor alpha is dispensable for the vasculoprotective actions of 17beta-estradiol. *Proceedings of the National Academy of Sciences of the United States of America*. 2009;106:2053-2058
34. Toutain CE, Filipe C, Billon A, Fontaine C, Brouchet L, Guery JC, Gourdy P, Arnal JF, Lenfant F. Estrogen receptor alpha expression in both endothelium and hematopoietic cells is required for the accelerative effect of estradiol on reendothelialization. *Arterioscler Thromb Vasc Biol*. 2009;29:1543-1550
35. Kauffenstein G, Tamareille S, Prunier F, Roy C, Ayer A, Toutain B, Billaud M, Isakson BE, Grimaud L, Loufrani L, Rousseau P, Abraham P, Procaccio V, Monyer H, de Wit C, Boeynaems JM, Robaye B, Kwak BR, Henrion D. Central role of p2y6 udp receptor in arteriolar myogenic tone. *Arterioscler Thromb Vasc Biol*. 2016;36:1598-1606
36. Begorre MA, Dib A, Habchi K, Guihot AL, Bourreau J, Vessieres E, Blondeau B, Loufrani L, Chabbert M, Henrion D, Fassot C. Microvascular vasodilator properties of the angiotensin ii type 2 receptor in a mouse model of type 1 diabetes. *Sci Rep*. 2017;7:45625
37. Robinet P, Milewicz DM, Cassis LA, Leeper NJ, Lu HS, Smith JD. Consideration of sex differences in design and reporting of experimental arterial pathology studies-statement from atvb council. *Arterioscler Thromb Vasc Biol*. 2018;38:292-303
38. Daugherty A, Tall AR, Daemen M, Falk E, Fisher EA, Garcia-Cardena G, Lusis AJ, Owens AP, 3rd, Rosenfeld ME, Virmani R, American Heart Association Council on Arteriosclerosis T, Vascular B, Council on Basic Cardiovascular S. Recommendation on design, execution, and reporting of animal

atherosclerosis studies: A scientific statement from the american heart association. *Arterioscler Thromb Vasc Biol*. 2017;37:e131-e157
39. Tarhouni K, Guihot AL, Freidja ML, Toutain B, Henrion B, Baufreton C, Pinaud F, Procaccio V, Grimaud L, Ayer A, Loufrani L, Lenfant F, Arnal JF, Henrion D. Key role of estrogens and endothelial estrogen receptor alpha in blood flow-mediated remodeling of resistance arteries. *Arterioscler Thromb Vasc Biol*. 2013;33:605-611
40. Vion AC, Kheloufi M, Hammoutene A, Poisson J, Lasselin J, Devue C, Pic I, Dupont N, Busse J, Stark K, Lafaurie-Janvore J, Barakat AI, Loyer X, Souyri M, Viollet B, Julia P, Tedgui A, Codogno P, Boulanger CM, Rautou PE. Autophagy is required for endothelial cell alignment and atheroprotection under physiological blood flow. *Proceedings of the National Academy of Sciences of the United States of America*. 2017;114:E8675-E8684
41. O'Brien JE, Peterson TJ, Tong MH, Lee EJ, Pfaff LE, Hewitt SC, Korach KS, Weiss J, Jameson JL. Estrogen-induced proliferation of uterine epithelial cells is independent of estrogen receptor alpha binding to classical estrogen response elements. *J Biol Chem*. 2006;281:26683-26692
42. Guetta V, Quyyumi AA, Prasad A, Panza JA, Waclawiw M, Cannon RO, 3rd. The role of nitric oxide in coronary vascular effects of estrogen in postmenopausal women. *Circulation*. 1997;96:2795-2801
43. Wyckoff MH, Chambliss KL, Mineo C, Yuhanna IS, Mendelsohn ME, Mumby SM, Shaul PW. Plasma membrane estrogen receptors are coupled to endothelial nitric-oxide synthase through galpha(i). *J Biol Chem*. 2001;276:27071-27076
44. Guivarc'h E, Buscato M, Guihot AL, Favre J, Vessieres E, Grimaud L, Wakim J, Melhem NJ, Zahreddine R, Adlanmerini M, Loufrani L, Knauf C, Katzenellenbogen JA, Katzenellenbogen BS, Foidart JM, Gourdy P, Lenfant F, Arnal JF, Henrion D, Fontaine C. Predominant role of nuclear versus membrane estrogen receptor alpha in arterial protection: Implications for estrogen receptor alpha modulation in cardiovascular prevention/safety. *J Am Heart Assoc*. 2018;7
45. Billon-Gales A, Krust A, Fontaine C, Abot A, Flouriot G, Toutain C, Berges H, Gadeau AP, Lenfant F, Gourdy P, Chambon P, Arnal JF. Activation function 2 (af2) of estrogen receptor-alpha is required for the atheroprotective action of estradiol but not to accelerate endothelial healing. *Proceedings of the National Academy of Sciences of the United States of America*. 2011;108:13311-13316
46. Hamilton KJ, Arao Y, Korach KS. Estrogen hormone physiology: Reproductive findings from estrogen receptor mutant mice. *Reprod Biol*. 2014;14:3-8
47. Bernelot Moens SJ, Schnitzler GR, Nickerson M, Guo H, Ueda K, Lu Q, Aronovitz MJ, Nickerson H, Baur WE, Hansen U, Iyer LK, Karas RH. Rapid estrogen receptor signaling is essential for the protective effects of estrogen against vascular injury. *Circulation*. 2012;126:1993-2004
48. Lu Q, Pallas DC, Surks HK, Baur WE, Mendelsohn ME, Karas RH. Striatin assembles a membrane signaling complex necessary for rapid, nongenomic activation of endothelial no synthase by estrogen receptor alpha. *Proceedings of the National Academy of Sciences of the United States of America*. 2004;101:17126-17131
49. Chambliss KL, Simon L, Yuhanna IS, Mineo C, Shaul PW. Dissecting the basis of nongenomic activation of endothelial nitric oxide synthase by estradiol: Role of eralpha domains with known nuclear functions. *Mol Endocrinol*. 2005;19:277-289
50. Chauhan S, Jelen F, Sharina I, Martin E. The g-protein regulator lgn modulates the activity of the no receptor soluble guanylate cyclase. *The Biochemical journal*. 2012;446:445-453
51. Wu CH, Chang GY, Chang WC, Hsu CT, Chen RS. Wound healing effects of porcine placental extracts on rats with thermal injury. *Br J Dermatol*. 2003;148:236-245
52. Rockwell LC, Pillai S, Olson CE, Koos RD. Inhibition of vascular endothelial growth factor/vascular permeability factor action blocks estrogen-induced uterine edema and implantation in rodents. *Biol Reprod*. 2002;67:1804-1810
53. Billon A, Lehoux S, Lam Shang Leen L, Laurell H, Filipe C, Benouaich V, Brouchet L, Dessy C, Gourdy P, Gadeau AP, Tedgui A, Balligand JL, Arnal JF. The estrogen effects on endothelial repair and mitogen-activated protein kinase activation are abolished in endothelial nitric-oxide (no) synthase knockout mice, but not by no synthase inhibition by n-nitro-l-arginine methyl ester. *The American journal of pathology*. 2008;172:830-838
54. Elhage R, Bayard F, Richard V, Holvoet P, Duverger N, Fievet C, Arnal JF. Prevention of fatty streak formation of 17beta-estradiol is not mediated by the production of nitric oxide in apolipoprotein e-deficient mice. *Circulation*. 1997;96:3048-3052
55. Hodgin JB, Knowles JW, Kim HS, Smithies O, Maeda N. Interactions between endothelial nitric oxide synthase and sex hormones in vascular protection in mice. *The Journal of clinical investigation*. 2002;109:541-548

56. Fredette NC, Meyer MR, Prossnitz ER. Role of gper in estrogen-dependent nitric oxide formation and vasodilation. *The Journal of steroid biochemistry and molecular biology*. 2018;176:65-72
57. Barton M, Prossnitz ER. Emerging roles of gper in diabetes and atherosclerosis. *Trends in endocrinology and metabolism: TEM*. 2015;26:185-192
58. Kumar P, Wu Q, Chambliss KL, Yuhanna IS, Mumby SM, Mineo C, Tall GG, Shaul PW. Direct interactions with g alpha i and g betagamma mediate nongenomic signaling by estrogen receptor alpha. *Mol Endocrinol*. 2007;21:1370-1380

Figure legends:

Figure 1: ***R264A-ERα*** **female mice present a normal reproductive tract.**
A) Representation of the structural domains and position of the R264 within murine ERα. B) Estrous cycles in WT and *R264A-ERα* mice**.** A typical estrous cycle profile is shown for each genotype (upper panel). E= Estrus; P = Proestrus; M-D= Metestrus+Diestrus.*; n=8/group*. C) Histological observation of ovarian function in WT and *R264A-ERα* mice**.** Representative pictures of adult ovaries are shown for each genotype. Scale bar = 1mm.

Figure 2: Uterine weight is maintained in ***R264A-ERα*** **mice while acute proliferative response to E2 is increased at 24 hours.**
A) **Representative images of intact uteri from WT and** ***R264A-ERα*** **mice**
B) **Uterine wet weight** (mean ± SEM, n=8 for each genotype). Unpaired t-test with Welch's correction was used. ns: not significant between WT-ERα versus *R264-ERα* mice
C) **Expression of ERα in uteri from WT and** ***R264A-ERα*** **mice**, as detected by Western blot using anti-ERα antibody (60C) and β-actin as a loading control.
D) **Relative expression of ERα in uteri of WT and** ***R264A-ERα*** **to β-actin** as loading control. (n=6 for each genotype). Unpaired t-test with Welch's correction was used. ns: not significant between WT-ERα versus *R264-ERα* mice
E) **ERα immunodetection in stromal and epithelial compartments from transverse uterus sections** in WT **and** ***R264A-ERα*** **mice** with higher magnification on the middle panels. Scale bar= 50µm.
F) **Uterine wet weights in ovariectomized WT and** ***R264A-ERα*** **mice** injected s.c with vehicle (Veh, castor oil) or 17β-estradiol (E2, 8µg/kg) and euthanized 24 hours after treatment. The number of mice are mentionned on the botton of the bar. Two-way ANOVA followed by Bonferroni post-test was performed (Interaction: *) - A significant effect of E2 was found between WT and *R264A-ERα* (*, $P<0.05$).
G) **Representative Ki-67 immmunodetection**.
H) **Percentages of Ki-67 positive cells in epithelium** 24 hours after s.c E2 injection in uteri of *R264A-ERα* and WT mice as compared to placebo treated mice. The number of mice are mentionned on the botton of the bar. Two-way ANOVA followed by Bonferroni post-test was performed (Interaction: *) - A significant effect of E2 was found between WT and *R264A-ERα* (**, $P<0.01$).

Figure 3: Large scale analysis on response to E2 in the uterus of ***R264A-ERα*** **mice as compared to its control littermates.** Gene expression profiles were obtained by microarray

analysis (DN Agilent SurePrint G3 Mouse GE 8x60K) of uterine samples from WT and *R264A-ERα* mice treated with E2 (8 µg/kg, 6 h) or vehicle (Veh), n = 4.
A) Two-dimensional representation of log2-expression ratios, comparing *R264A-ERα* treated E2 versus vehicle (y-axis) with WT treated E2 versus vehicle (x-axis).
B) Heat map representing the data obtained on WT and *R264A-ERα* samples (BH adjusted P < 0.05).
C) Venn diagram illustrating the overlaps between the genes significantly (FC > 1.5 with BH adjusted *P*val < 0.05) differentially regulated in the uterus by E2 in WT and *R264A-ERα* and between the two genotypes in response to E2.
D) Table summarizing the genes identified as being differentially regulated (absolute FC > 1.5) between both genotypes in the presence of E2, with a BH correction of *P*values on either unfiltered probes expression (Pval1, as done in panel E) or on probes first filtered upon their expression levels (Pval2). Significant (*P*< 0.05) *P*val1 and *P*val2 are shown in bold.
E) Normalized relative mRNA levels in uteri from ovariectomized WT and *R264A-ERα* mice treated acutely (6h) with E2 (8 µg/kg) or with vehicle. Statistical analyses (*2-way Anova)* were performed on ΔΔCq (log2) data. For all genes a significant interaction was revealed between the 2 main effects. The indicated effects are post-hoc based (Bonferroni correction). The data shown are geometrical means of relative quantities ($2^{-\Delta\Delta Cq}$ +/- linearized log2-based SEM) n=4/group.

<u>Figure 4: Rapid vascular effects of E2 such as rapid dilation are lost with the mutation R264A of ERα in female mice.</u>
A) Expression of ERα in primary endothelial cells (ECs) at passage PO isolated from aorta of WT and R264A mice, as detected by Western blot using anti-ERα antibody (60C) **.** Uteri from WT mice was loaded as positive control and stain free staining of the membrane after transfer was performed as loading control of total protein. MW: Molecular weight.
B)Quantitative analysis of expression level of ERα in primary endothelial cells at passage P0 from aorta from WT and R264A-ERα mice , expressed as a ratio to the total loaded protein as detected using stain free of the membrane (n=3 for each genotype).
C) Typical tracings obtained for dilation of mesenteric arteries cannulated in vitro under a pressure of 75 mmHg) in a arteriograph from WT and *R264A-ERα* female mice following increased concentration of E2 (0.01 to 1µM) diluted in ethanol (EtOH, 1/10000, 1/10000 and 1/1000 respectively), added to the bath and after precontraction with phenylephrine
D) Percentages of dilation of mesenteric arteries from female WT and *R264A-ERα* mice following addition of E2 (0.01 to 1µM)- Results of 2-way Anova was shown, explaining the effect of both variables (Treat.= E2 treatment ; Gen.=Genotype) and their interaction *(Inter.))* . As an interaction was observed between the 2 factors (P<0.0001), Bonferroni post-tests were then performed. A significant effect of E2 was found in the WT-ERα at 10^{-7} and 10^{-6} (* (*P*<0.05) and *** (*P*<0.001) respectively), but not in *R264A-ERα*. A significant difference was also found between WT-E2 with R264A-ERα-E2 at 10^{-7} and 10^{-6} ($$ (*P*<0.01) and $$$ (*P*<0.001) respectively).
E) Percentages of E2-mediated dilation of mesenteric arteries from female WT and *R264A-ERα* mice previously incubated with L-NNA (100 µM) during 30 min. These results were compared to the results obtained for ERα-WT-E2 and *R264A-ERα*-E2, shown in panel D. A 2-way Anova was performed between these 4 groups and an interaction was observed between the 2 factors (P_{inter}*: ****** **)**. The effect of treatment then was studied in each genotype using Bonferroni post-test. WT-E2 versus WT-LNNA-E2 at 10^{-7} and 10^{-6} were significantly different (**, *P*<0.01) and (***, *P*<0.001) *respectively).*
F) Percentages of acetylcholine (1 µM)-mediated dilation of mesenteric resistance arteries *in vitro* from female WT-ERα or *R264A-ERα* mice measured in the presence and

absence of L-NNA in the same groups. (n=5 and 8 for WT-Ac and *R264A-ERα*, respectively and n=5 and 5, for WT+L-NNA and *R264A-ERα*+L-NNA, respectively. Results of 2-way anova was shown

G) Percentages of E2-mediated dilation of mesenteric arteries from female WT and R264A-ERα mice previously incubated with pertussis Toxin (PTX) during 120 min. A control was also performed with ethanol with the same time of incubation. A 2-way Anova was performed between these 3 groups and an interaction was observed between the 2 factors (*P_{inter}: P=0.001*, ** **)**. The effect of treatment was studied in each genotype using Bonferroni post-test. WT-E2 versus WT-PTX-E2 were significantly different at 10^{-7} and 10^{-6}, respectively ((*, *P*<0.05) and (**, *P*<0.01)). WT-E2 as significantly different than WT-EtHOH at 10^{-6} ($$, *P*<0.01).

Figure 5: E2-induced acceleration of reendothelialization are lost with the mutation R264A of ERα in female mice.

A) **Carotid artery reendothelialization** in ovariectomized WT and *R264-ERα* mice treated or not with E2 (80 µg/Kg/d, 2 wk). Representative photographs of blue evans staining of re-endothelialization are shown (right panel) and corresponding quantification (left panel). (n=9 and 10 for WT-PLB and WT-E2, respectively and n=7 and 8, for *R264-ERα* PLB and E2, respectively). As the 2-way Anova revealed an interaction between E2 treatment and genotype (Interaction: *), Bonferroni post-test was performed. A significant effect of E2 was found in the WT-ERα (***, *P*<0.001).

B) Carotid artery reendothelialization in ovariectomized WT reconstituted with hematopoietic cells from WT or *R264-ERα* mice treated or not with E2 (80 µg/Kg/d, 2 wk). (n=6 and 7 for WT-PLB and WT-E2, respectively and n=7 and 5, for R264-ERα PLB and E2, respectively). (*2-way Anova:* interaction (Inter.) E2 treatment (Treat); Genotype (Gen).

Figure 6: R264A-ERα female mice conserve nuclear protective vascular actions of E2 in aorta preventing atherosclerosis in LDLR$^{-/-}$ mice and maintained arterial remodeling in mesenteric arteries.

A) Normalized relative mRNA levels in aorta from ovariectomized WT and R264A mice treated acutely (6h) with E2 (8 µg/kg) or with vehicle (Veh). Statistical analyses (*2-way Anova)* were performed on ΔΔCq (log2) data. The *P* values for the 2 main effects and their interaction are given in the box. The data shown are geometrical means of relative quantities ($2^{-\Delta\Delta Cq}$ +/- linearized log2-based SEM) n=6/group.

B) Representative images and C) quantification of lipid deposition at the aortic sinus in WT LDLR-/- and *R264-ERα LDLR-/-* mice after red oil staining. (n=9 and 6 for WT-PLB and WT-E2, respectively and n=15 and 9, for *R264-ERα* PLB and E2, respectively). Results of 2-way anova was shown.

D) Schematic representation of the protocol used to induce the flow-mediated remodeling of mesenteric arteries *in vivo* (see Materials and Methods). Following ligation of some 2nd order mesenteric arteries downstream the 1st order mesenteric arteries, 1st order arteries with ligation are submitted chronically to high flow (HF) and compared to the 1st order mesenteric arteries without ligation (normal flow, NF)

E) Flow-mediated remodeling was then evaluated in mesenteric arteries isolated from WT and R264A mice in response to stepwise increases in pressure over 2 weeks (n= 4 for WT-ERα and 5 for *R264A-ERα*). Arterial diameter was measured *ex vivo* in response to stepwise increases in pressure in mesenteric arteries initially submitted chronically to high flow (HF) or normal flow (NF).). As the 2-way Anova revealed an interaction between E2 treatment and Genotype (Interaction: ****, *P*<0.001), Bonferroni post-test was performed. A significant effect of E2 was found in the *WT-ERα* (****, *P*<0.001). A significant effect in

remodeling was found between NF and HF in both WT and R264A-ERα mice at 50 and 75 mmHg (* and $, $P<0.05$) and at 100 and 125 mmHg (** , $P<0.01$ and $, $P<0.05$, respectively) . No significant difference was found between HF-WT and *HF-R264A-ERα* and NF-WT and *NF-R264A-ERα* .

Table 1: Serum levels of Estradiol, Testosterone and Progesterone (n=18) and Luteinezing hormone (LH) and Follicle-Stimulating Hormone (FSH) in WT and *R264A-ERα* mice. LH and FSH measurements were performed in estrus phase (n=8). *ns: non-significantly different from WT (*Mann Whitney test was used and no significant difference was found between genotypes).

.

	Estradiol (pg/ml)	Progesterone (pg/ml)	Testosterone (pg/ml)	LH (pg/ml)	FSH (pg/ml)
ERα-WT females	3.1 ±0,7	2790 ± 415	10.56 ± 415	205 ± 55	2993 ± 681
R264A-ERα females	2.2 ±0,6	2153 ±282	11.27 ±3.2	290 ±67	2102 ±860

Table 2: Body and uterine weights with plasmatic lipid (total cholesterol and HDL cholesterol) profiles and Oil Red O area (ORO) area in representative sections of aortic sinus of WT LDLR$^{-/-}$ and *R264A-ERα* LDLR$^{-/-}$ mice fed for 12 weeks with a hypercholesterolemic-atherogenic diet (mean± SEM, n=X). Results of 2-way Anova between the genotype and treatment are indicated on the right column of the Table.

	Arg$^{+/+}$ LDLr$^{-/-}$		Arg$^{-/-}$ LDLr$^{-/-}$		P, two-factor ANOVA		
	Ctrl (n=10)	E_2 (n=7)	Ctrl (n=16)	E_2 (n=9)	Genotype	E_2	Interaction
Body weight (g)	23.5 ± 1.3	21. ± 0.8	24.1 ± 0.5	20.4 ± 0.6	-	** p=0.0033	NS
Uterine weight (mg)	7.1 ± 0.5	160 ± 18	7.5 ± 0.3	163 ± 41	-	**** p<0.0001	NS
Total Chol. (mg/dL)	1390 ± 33	828 ± 116	1668 ± 173	950 ± 73	-	** p=0.0038	NS
HDL Chol. (mg/dL)	38.3 ± 4.5	41.6 ± 1.7	41.3 ± 3.7	43.7 ± 4.2	-	-	NS
ORO area (x10^3 µm^2)	235.3 ± 15.9	38.3 ± 10.1	179.2 ± 18.6	21.4 ± 4.1	-	**** P<0.0001	NS

Highlights:

- Mutation of Arginine 264 of Estrogen receptor ERα abrogated acceleration of re-endothelialization and rapid arteriolar remodeling in response to E2
- In contrast, vasculoprotective effects of E2 such as prevention of atheroma or arterial remodeling, known to be mediated by nuclear actions of ERα are conserved
- R264A-ERα mouse is the first fertile mouse model harboring a single mutation of ERα with specific loss-of function of rapid ERα signaling in vascular functions.

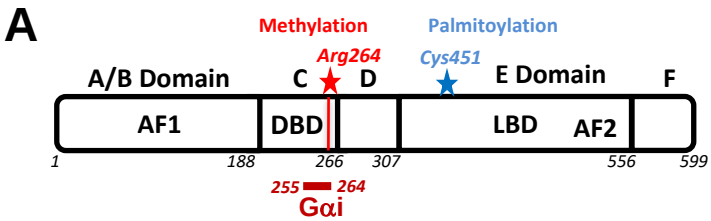

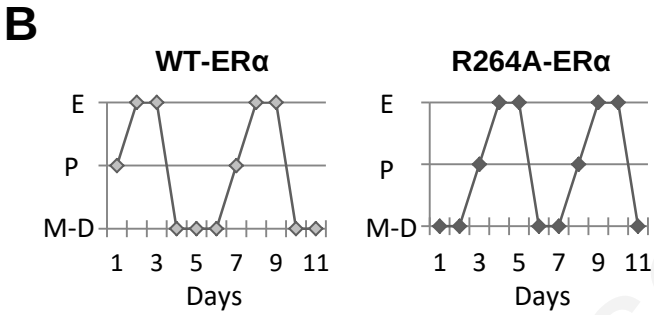

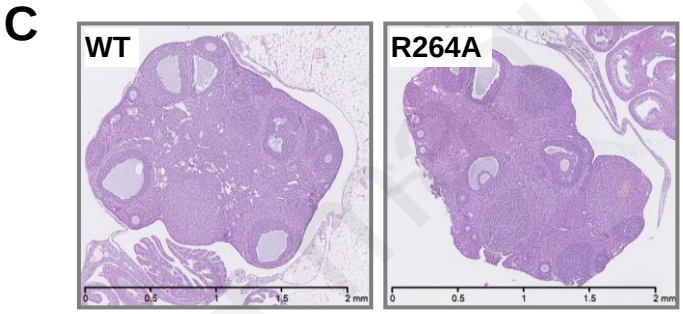

Figure 1

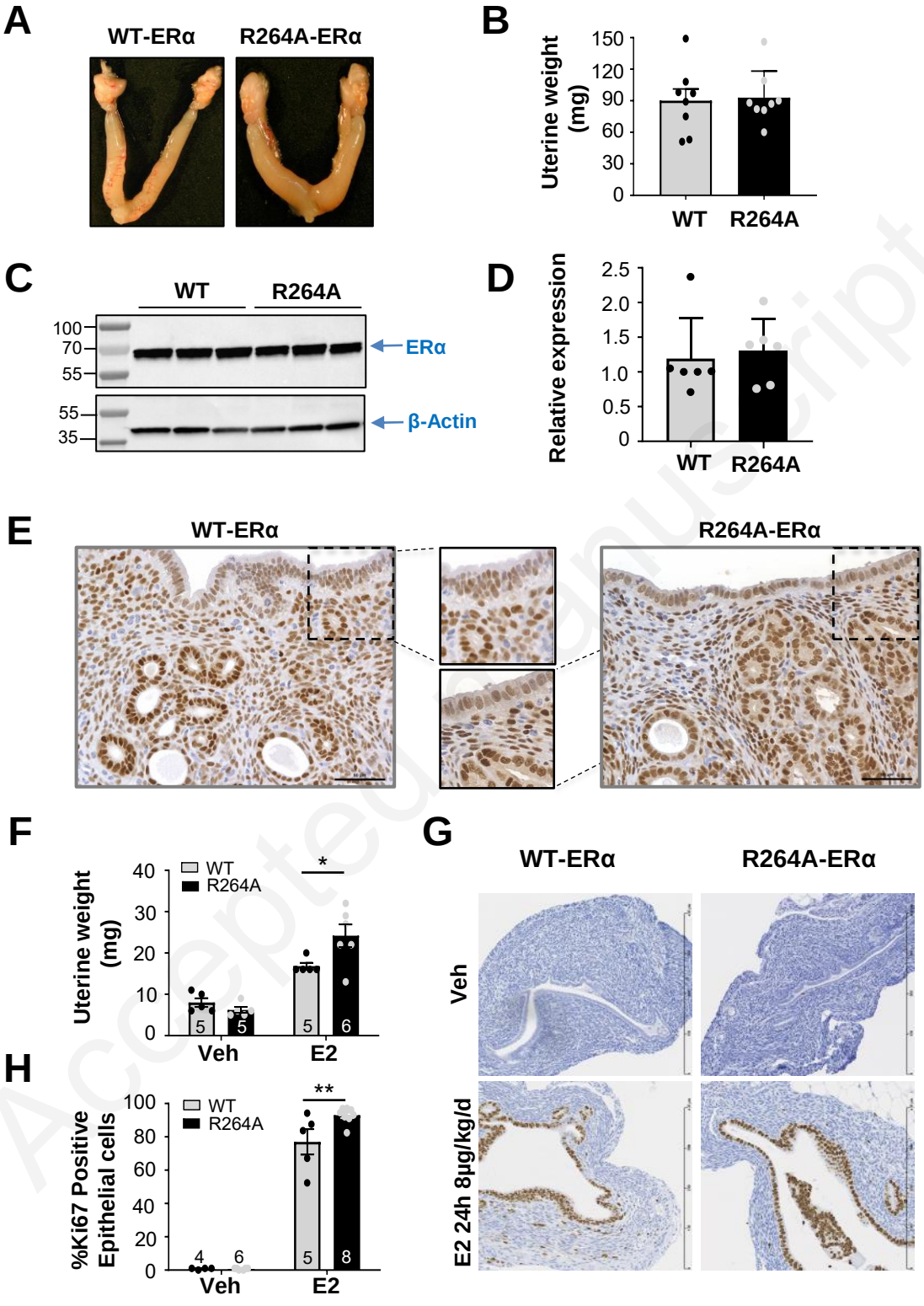

Figure 2

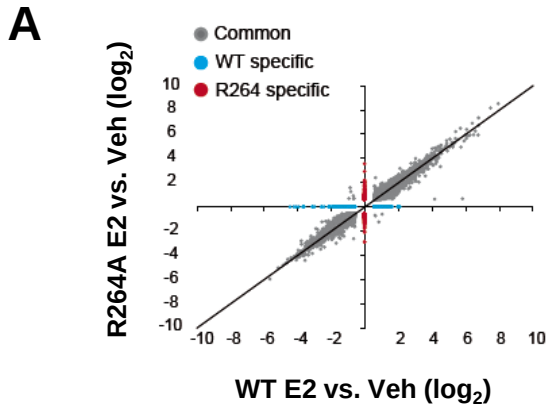

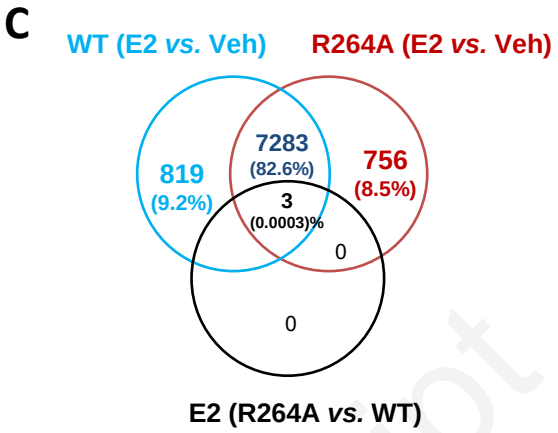

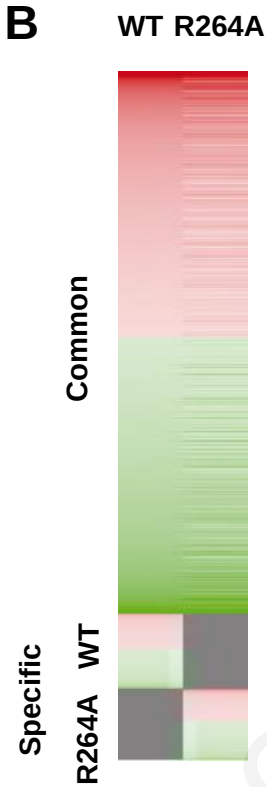

D

Gene	Transcript	Log_2 FC (E2 R264A vs. WT)	*P*val1	*P*val2
Fam178b	NM_201365	-0.9451	0.0168	0.0331
Gpsm2	NM_029522	-0.7127	0.0438	0.0688
Il11	NM_008350	0.8931	0.0002	0.0152
Nmur2	NM_153079	-0.7192	0.2426	0.0074
Tmem190	NM_030028	0.8794	0.7937	0.0431
Kalrn	NM_177357	0.6203	0.1054	0.1162

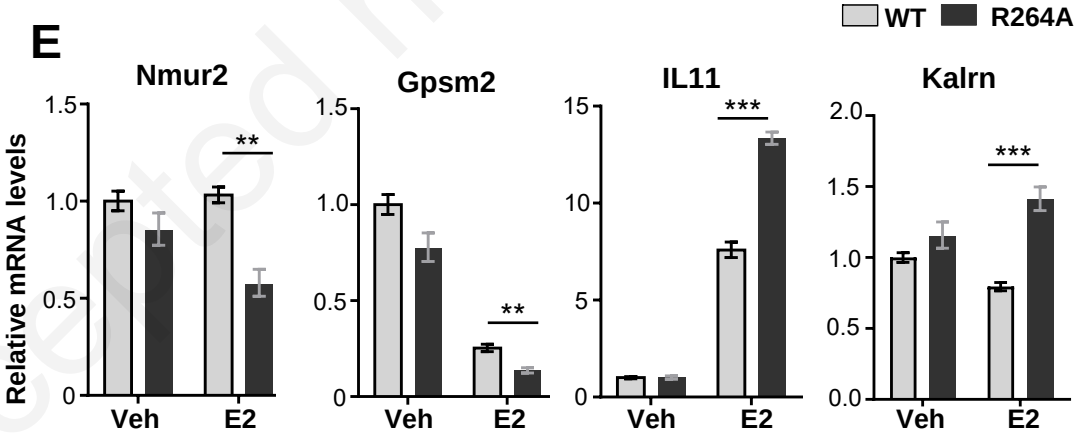

Figure 3

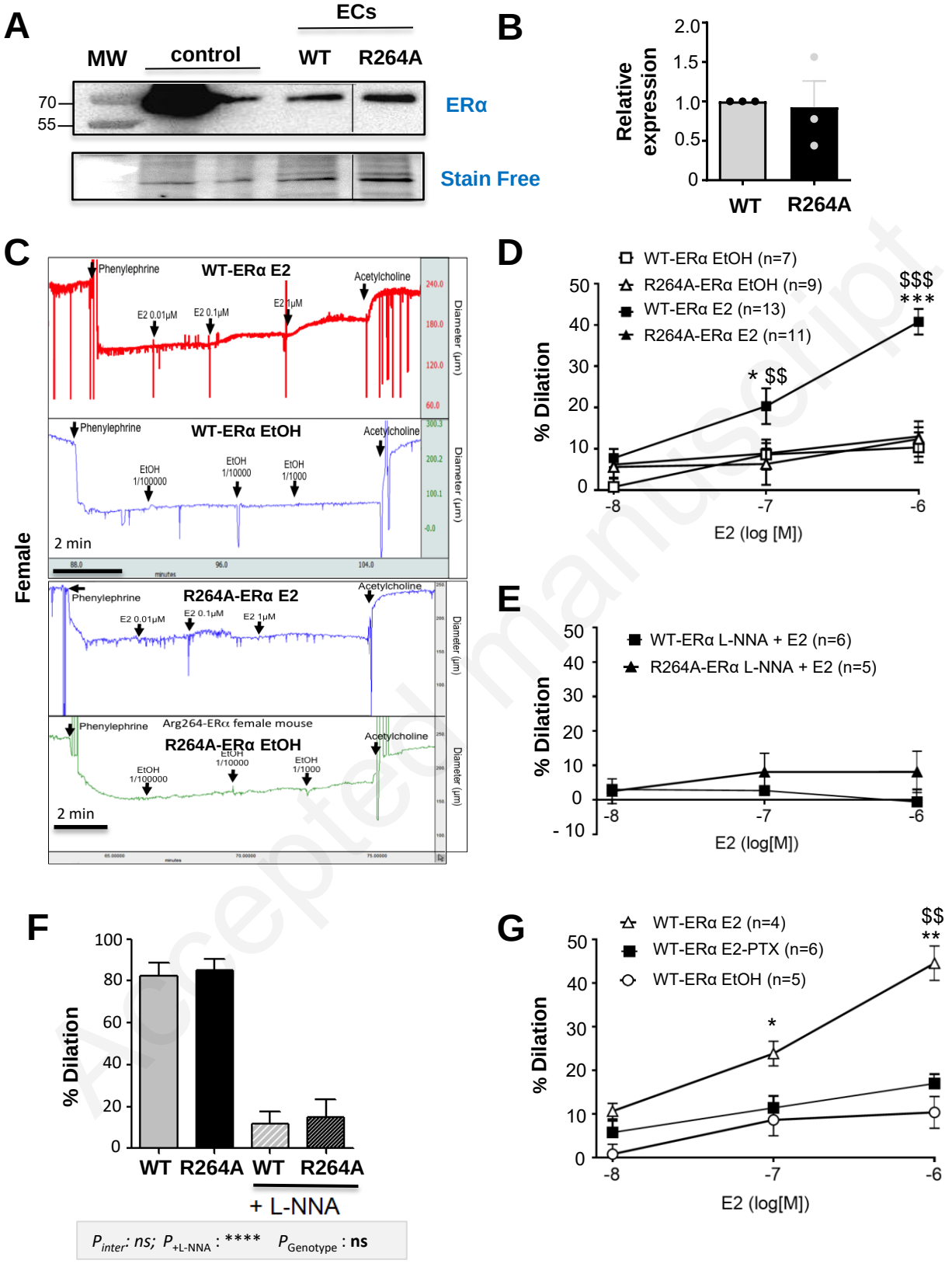

Figure 4

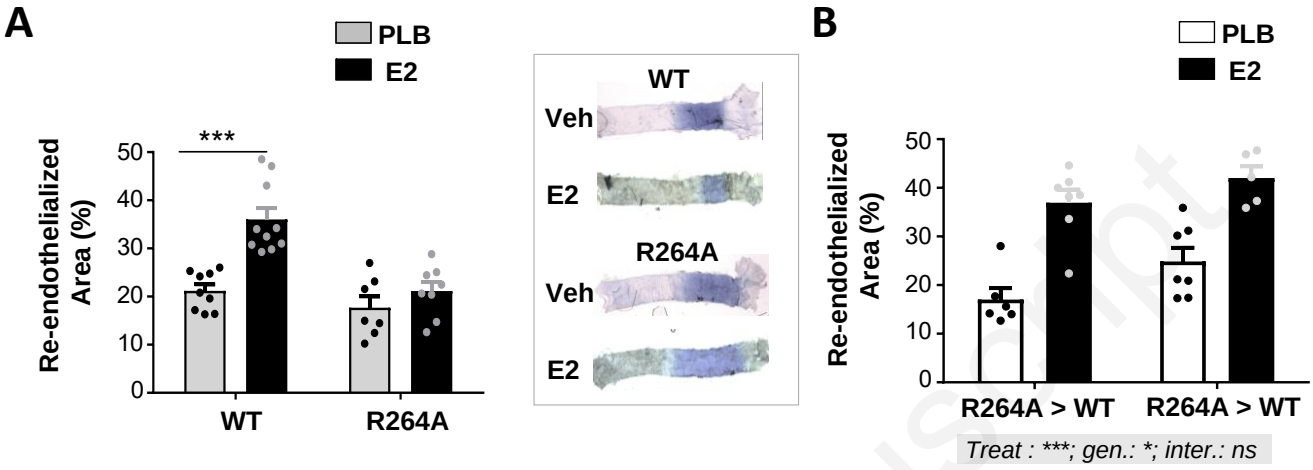

Figure

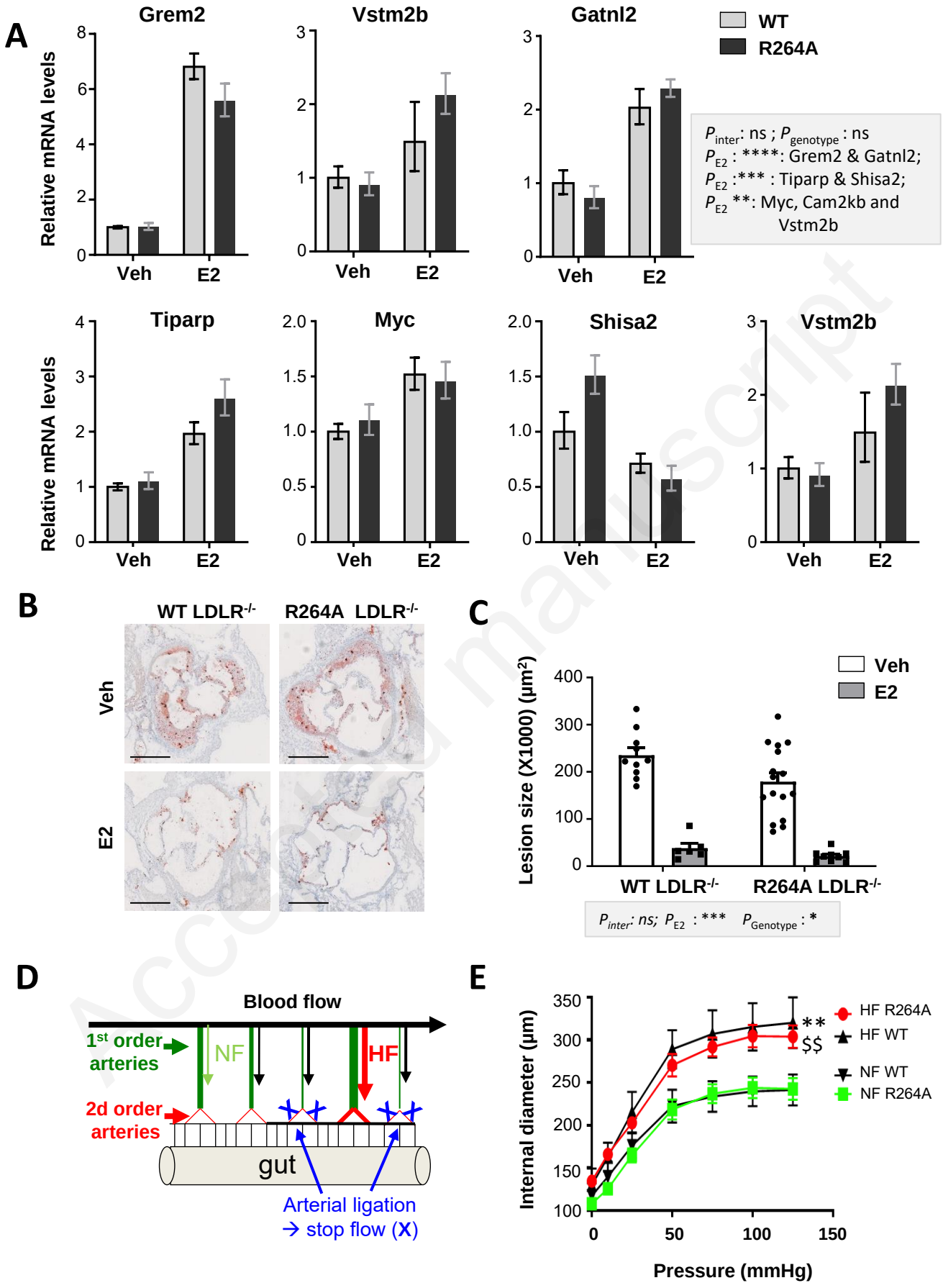
A
Grem2
Vstm2b
Gatnl2
WT
R264A
Relative mRNA levels
Veh
E2
P_{inter}: ns ; $P_{genotype}$: ns
P_{E2} : ****: Grem2 & Gatnl2;
P_{E2} :*** : Tiparp & Shisa2;
P_{E2} **: Myc, Cam2kb and Vstm2b
Tiparp
Myc
Shisa2
Vstm2b
B
WT LDLR-/-
R264A LDLR-/-
Veh
E2
C
Veh
E2
Lesion size (X1000) (µm²)
WT LDLR-/-
R264A LDLR-/-
P_{inter}: ns; P_{E2} : *** $P_{Genotype}$: *
D
Blood flow
1st order arteries
2d order arteries
NF
HF
gut
Arterial ligation
→ stop flow (X)
E
Internal diameter (µm)
Pressure (mmHg)
HF R264A
HF WT
NF WT
NF R264A
**
$$

Figure 6